

# Novel polyamide 12 based nanocomposites for industrial applications

A. Dorigato<sup>1</sup> · M. Brugnara<sup>2</sup> · A. Pegoretti<sup>1</sup>

Received: 30 January 2017 / Accepted: 15 May 2017  
© Springer Science+Business Media Dordrecht 2017

**Abstract** In this paper novel electro-active polyamide 12 (PA12) based nanocomposites were prepared through melt compounding by adding different kinds of carbonaceous nanofillers. The thermo-electrical properties of the bulk samples were then compared with those of the corresponding fibers. FESEM images highlighted a homogeneous dispersion of carbon black (CB) and carbon nanofibers (CNF) within the matrix, while exfoliated graphite nanoplatelets (xGnP) based nanocomposites showed an aggregated morphology. A slight increase of the glass transition and of the crystallization temperature was evidenced by DSC tests, while thermogravimetric analysis showed an improvement of the thermal degradation resistance. Nanofiller addition promoted substantial increments of the elastic modulus coupled with an electrical resistivity drop up to  $10^3 \Omega \text{ cm}$ , with interesting synergistic effects for nanocomposites filled with both CB and CNF. FESEM micrographs on the fibers demonstrated how the drawing process promoted the breakage of CB aggregates and their alignment along the drawing direction, leading to an increase of both the elastic and failure properties with respect to the neat fibers. On the other hand, nanofiller orientation led to an electrical resistivity enhancement of two orders of magnitude with respect to the corresponding bulk

materials, and a CB amount of 10 wt% was thus required to observe a sensible fiber heating upon voltage application.

**Keywords** Polyamide · Nanocomposites · Electrical resistivity · Fibers

## Introduction

It has been widely recognized that nanoscale effects in polymer matrix nanocomposites can significantly affect the physical properties of plastics in terms of elastic modulus [1], impact behaviour [2], thermal degradation and fire resistance [3–6]. It is also clear that traditional polymer matrices are generally characterized by a limited electrical conduction capability [7], but several methods can be applied to prepare electrically conductive polymers [8, 9]. The addition of conductive fillers such as carbon black (CB), carbon nanotubes (CNTs), exfoliated graphite nanoplatelets (xGnP) or metal particles to polymers is probably the most promising technique, and several electro-active nanocomposite systems were recently developed by our research group [10–14]. Above a critical filler concentration (i.e. percolation threshold), a conductive path within the polymer matrix constituted by a network of filler particles aggregates can be formed [15–17]. These materials find a wide application in films for packaging of sensitive electronics components, where charge dissipation and electrical conductivity are key technological requirements. In these materials, the achievements of a good filler dispersion quality represents one of the most critical issues, and an inhomogeneous dispersion can determine serious technical problems such as heavy process dependency.

✉ A. Dorigato  
andrea.dorigato@unitn.it

✉ A. Pegoretti  
alessandro.pegoretti@unitn.it

<sup>1</sup> Department of Industrial Engineering and INSTM Research Unit, University of Trento, Via Sommarive 9, 38123 Trento, Italy

<sup>2</sup> UFI Innovation Center Srl, Corso Trento 20 38061, Ala, Italy

Starting from 1935, polyamides received both scientific and industrial attention, because of the possibility of developing fibers and bulk materials with elevated technological properties. After nylon 6,6 and nylon 6, other kinds of aliphatic polyamides have been produced. Among them, nylon 11, nylon 12, and nylon 6,10 have become of specialized interest as plastics materials [18, 19]. Thanks to the higher methylene/amide ratio (11/1), nylon 12 (PA12) is endowed with a lower melting temperature (about 180 °C) with respect to PA66 (10/2). In the last 50 years, PA12 has been utilized as replacement of commodity nylons in every primary polymer process, including extrusion, injection molding and blow molding [20]. Moreover, the preparation of PA12 based blends and composites has been widely considered in literature. For instance, uncompatibilized and compatibilized blends based on polyamide 12 (PA12) and isotactic polypropylene (PP) were investigated by Jose [21] and Tang [22]. Microfibrillar reinforced composites were developed by Sarkissova et al. [23] through a reactive melt extrusion of PET and polyamide 12 in the presence of a catalyst. Several examples can be found in literature about the characterization of PA12 based nanocomposites prepared to enhance the physical properties of neat polyamide 12. In most of these works, organically modified clays were considered [24–27]. In our previous papers on polyamide 12 composites, it was demonstrated the possibility to reinforce this polymer matrix with polyamide 66 recycled fibers [28] and aramid regenerated fibers [29]. In both cases, interesting improvements of the thermo-mechanical properties with respect to the neat PA12 were detected.

Polyamide 12 can be applied in the production of injection molded parts, but it can also be extruded in sheets, films, profiles or in non-woven fabrics. Due to their low cost and high efficiency, polymeric non-woven fabrics are extensively applied in air and liquid filters for the automotive field and industrial equipment [30]. Thanks to their elevated porosity, large surface area, dust-free, low-cost, easy processability and modifiability, these products can be also applied for hygiene, family and medical use. From a microstructural point of view, nonwovens are constituted by thin fibres assembled together to form a web and can be manufactured through different processes (i.e. wet- or air-laid, spunbond or meltblown). In a recent work of our group [30], an organo-modified clay (OMC) was additivated to a polyamide 6 (PA6) matrix at various concentrations during the polymerization stage or by melt compounding in a twin-screw extruder, and the resulting pellets were used for the production of depth filters in the shape of cylindrical nonwoven webs melt-blown. The effect of the nanofiller addition on the processability, the thermo-

mechanical properties and filterability capability of the prepared materials was investigated. The role of CB introduction of the physical properties of Nylon 12 based nanocomposites was partially investigated in the last years. For instance, Athreya et al. explored the possibility to process an electrically conductive polymer nanocomposite made of Nylon 12 reinforced with 4 wt% of CB through Selective Laser Sintering (SLS) technique [31]. It was demonstrated how carbon black filled Nylon-12 nanocomposites could be successfully made by SLS, with a reduction of the elastic modulus for the nanocomposite samples due to the formation of a segregated nanofiller structures and a weak polymer–filler interface. In another paper of Yanagizawa et al. the dependency of the electrical conductivity of CB filled Nylon-12 fibers on the spinning conditions was studied [32]. However, a systematic investigation of the role played by different kind of carbon based nanofillers on the thermo-electrical properties of Nylon 12 based nanocomposites has never been performed before.

Therefore, the objective of the present paper is the development and the thermo-electrical characterization of innovative PA12 based nanocomposites, filled with different kinds of commercial carbonaceous nanofillers (CB, CNTs and xGnP). This research was performed in collaboration with UFI Innovation Center Srl, an important producer of innovative fluid filters for the automotive sector. This work represent a part of an experimental activity focused on the development of innovative nanocomposite melt blown conductive filters, that could be heated through Joule effect at different voltages. The effect of the nanofiller addition on the physical properties of the bulk materials was analyzed. Furthermore, the properties of the bulk samples were compared with those of the fibers.

## Experimental part

### Materials

A Rilsan PA12, supplied by Arkema (Nanterre, France), was used as matrix (density 1.02 g/cm<sup>3</sup>, melting temperature 178 °C). Ketjenblack EC600JD carbon black (mean particles size 30 nm, BET surface area 1353 m<sup>2</sup>/g, density 1.95 g/cm<sup>3</sup>) was provided by Akzo Nobel Chemicals Spa (Arese, Italy). NanoAmor 1195JN vapour grown carbon nanofibers (density 1.78 g/cm<sup>3</sup>, BET specific surface area 28.8 m<sup>2</sup>/g, mean length 5–40 nm, core diameter 0.5–10 nm, outside diameter 240–500 nm) have been purchased by NanoAmor Inc. (Houston, TX, USA). Exfoliated graphite nanoplatelets (density 2.05 g/

cm<sup>3</sup>, purity 97 wt%) were supplied by XG Science Inc. (East Lansing, MI, USA).

### Samples preparation

Before to be used, all the materials have been dried in a Moretto X Dry Air drier at a temperature of 80 °C for 6 h with an air flow of 7 Nm<sup>3</sup>/h. Polymer granules and the filler were then melt-compounded for 5 min in a Thermo-Haake PolyLab Rheomix 600p at 200 °C and at a rotor speed of 50 rpm. The resulting materials were then hot-pressed at 200 °C for 5 min in a Carver Laboratory Press in order to obtain square sheets with a thickness between 1 and 1.2 mm, applying a pressure of 0.33 MPa. In order to avoid moisture absorption, all the sample were kept in a vacuum bag before the testing operations. In this way, CB, CNT and xGnP nanocomposites with filler concentrations between 0.5 and 6 wt% were prepared. In order to evaluate possible synergistic effects between the nanofillers, also nanocomposites samples containing both CB and CNF were prepared at different relative concentrations, keeping a total filler content of 4 wt%. In Table 1 the list of the prepared samples is reported.

For as concerns the preparation of polymer fibers, the prepared bulk materials were grinded and the resulting granules were utilized to feed an Estru 13 single screw extruder (Friul Filiere, Udine, Italy), with a L/d ratio of 15 and a screw diameter of 14 mm. A screw speed of 30 rpm and a temperature profile of 180/200/200/200 °C were utilized. In this way neat PA12, PA12-CB-3/CNF-1 and PA12-CB-10 nanocomposite fibers were prepared. The resulting filaments were then drawn at 100 °C at different draw ratios.

### Experimental methodologies

Microstructural features of the cryofractured surfaces of the prepared composites were investigated through a Zeiss Supra 40 field emission scanning electron

microscope (FESEM), equipped with an exclusive Gemini column.

DSC measurements were carried out with a Mettler DSC30 calorimeter. All the tests consisted of 3 ramps at 10 °C/min: a first heating from 0 °C to 250 °C, a cooling stage from 250 °C to 0 °C and a second heating from 0 °C to 250 °C. All the tests were performed under a nitrogen flow of 100 ml/min. The most important thermal properties of the materials, such as glass transition temperature ( $T_g$ ), melting temperature ( $T_m$ ) and crystallization temperature ( $T_c$ ), were determined. Moreover, the crystallinity content ( $X_c$ ) was computed by dividing the specific heat of fusion of the samples by the reference value of the melting enthalpy of fully crystalline PA12 (i.e. equal to 95 J/g [33]), taking into account the real weight fraction of PA12 in the composites. Thermostability of the prepared samples was studied through thermogravimetric analysis (TGA) by using a Mettler TG50 thermobalance under an air flow of 150 ml/min with a heating rate of 10 °C/min in the range 30–700 °C. The decomposition temperature ( $T_d$ ), taken as the temperature corresponding to the maximum mass loss rate, was determined.

Quasi-static tensile tests on bulk materials were performed on ISO 527 type 1BA samples (gage length 30 mm, width 5 mm, distance between the grips 55 mm, thickness 1.2 mm) by using an Instron 4502 tensile machine. The results represent the average value of at least five specimens. The elastic modulus was evaluated at ambient temperature as secant modulus between deformation levels of 0.05% and 0.25%. The tests were carried out at a crosshead speed of 0.25 mm/min imposing a maximum deformation of 1%. The strain was monitored through an Instron model 2620–601 resistance extensometer (gage length 12.5 mm). Tensile tests at break were performed at a crosshead speed of 50 mm/min without using the extensometer. In this way elastic modulus ( $E$ ), the maximum stress ( $\sigma_{max}$ ) and the strain at the maximum stress ( $\epsilon_{max}$ ) were determined. Tensile tests were also performed on neat PA12 and PA12-CB-3/CNF-1 nanocomposite fibers prepared at different draw ratios, by using an Instron 4502 tensile testing machine equipped with a load cell of 10 N. The gage length of the fibers was 30 mm. For the determination of the elastic modulus a crosshead speed of 1 mm/min was set, while tensile properties at break (UTS,  $\epsilon_{UTS}$ ) were determined at 50 mm/min. At least 5 specimens were tested for each sample.

Electrical volume resistivity measurements of bulk samples in direct current mode were carried out with a Keithley 6517A electrometer at room temperature. All the tests were conducted following the ASTM D257 standard on square film samples (length of 95 mm and thickness of 1 mm), by using coaxial electrodes in order to minimize the amount of current flowing through the surface. The bulk electrical resistivity ( $\rho$ )

**Table 1** List of the prepared samples

Sample code	Filler amount (wt%)	Sample type
PA12	-	bulk and fiber
PA12-CB-x	0.5 ÷ 6	bulk
PA12-CNF-x	0.5 ÷ 6	bulk
PA12-xGnP-x	0.5 ÷ 6	bulk
PA12-CB-1/CNF-3	1 CB – 3 CNF	bulk
PA12-CB-2/CNF-2	2 CB – 2 CNF	bulk
PA12-CB-3/CNF-1	3 CB – 1 CNF	bulk and fiber
PA12-CB-10	10	fiber

of the samples was computed through the expression reported in Eq. (1):

$$\rho = R \cdot \frac{\pi a^2}{t} \quad (1)$$

where  $R$  is the electrical resistance,  $a$  is the ray of the testing electrode,  $t$  is the thickness of the samples. Electrical resistivity of the fibers was measured applying the testing electrodes on the fibers at a distance of 30 mm. The evolution of the surface temperature upon voltage applications was measured both on bulk and on the fiber samples by using a Fluke TiRx thermographic camera. The tested bulk specimens were in the form of strips ( $35 \times 6 \times 1 \text{ mm}^3$ ), while the fibers were tested applying the electrodes at a distance of 30 mm. The surface temperatures was recorded at different time intervals starting from  $25 \text{ }^\circ\text{C}$ , applying voltage levels ranging from 10 V to 220 V.

## Results and discussion

### Characterization of bulk materials

It is well known that the macroscopic properties of polymer nanocomposites are strongly influenced by the quality of nanofiller dispersion within the matrix. Therefore, morphological features of the cryofractured surface of the prepared nanocomposites were investigated through FESEM analysis (see Fig. 1). Generally speaking, it is possible to state that both CB and CNF nanofillers are homogeneously dispersed within the matrix. This means that the shear stresses generated by the

mixer during the melt compounding were able to break the nanofiller aggregates and disperse them in the matrix with a good degree of homogeneity. The microstructure of the PA12-CB-4 nanocomposite is characterized by primary particles with a mean dimension of 40 nm, organized in aggregates of about 500 nm. These aggregates were formed during the manufacturing process and can not be broken [34]. On the other hand, in the PA12-CNF-4 sample nanofibers with a mean diameter of 75 nm homogeneously distributed within the matrix can be detected. It could be therefore expected that the good dispersion degree of both these nanofillers within the matrix could lead to the achievement of interesting thermal and electrical properties. In the case of PA12-xGnP-4 nanocomposite, a strong aggregation of the graphite lamellae is evident, and the mean dimension of these stacks is about 700 nm. This aggregation could negatively affect the physical properties of these composites. For as concerns the microstructural behaviour of nanocomposites with mixed composition, the microstructure is characterized by CB aggregates surrounded by single CNFs homogeneously distributed in the matrix. Such this microstructure could favour the formation of a conductive path within the material, thus promoting an improvement of the electrical conductivity.

Considering the future application of these materials as melt blown fabrics, the investigation of the influence of carbon based nanofillers on the thermal properties of the samples is of key importance. Therefore, DSC tests were performed on bulk nanocomposites. In Fig. 2a and in Fig. 2b representative DSC thermograms of

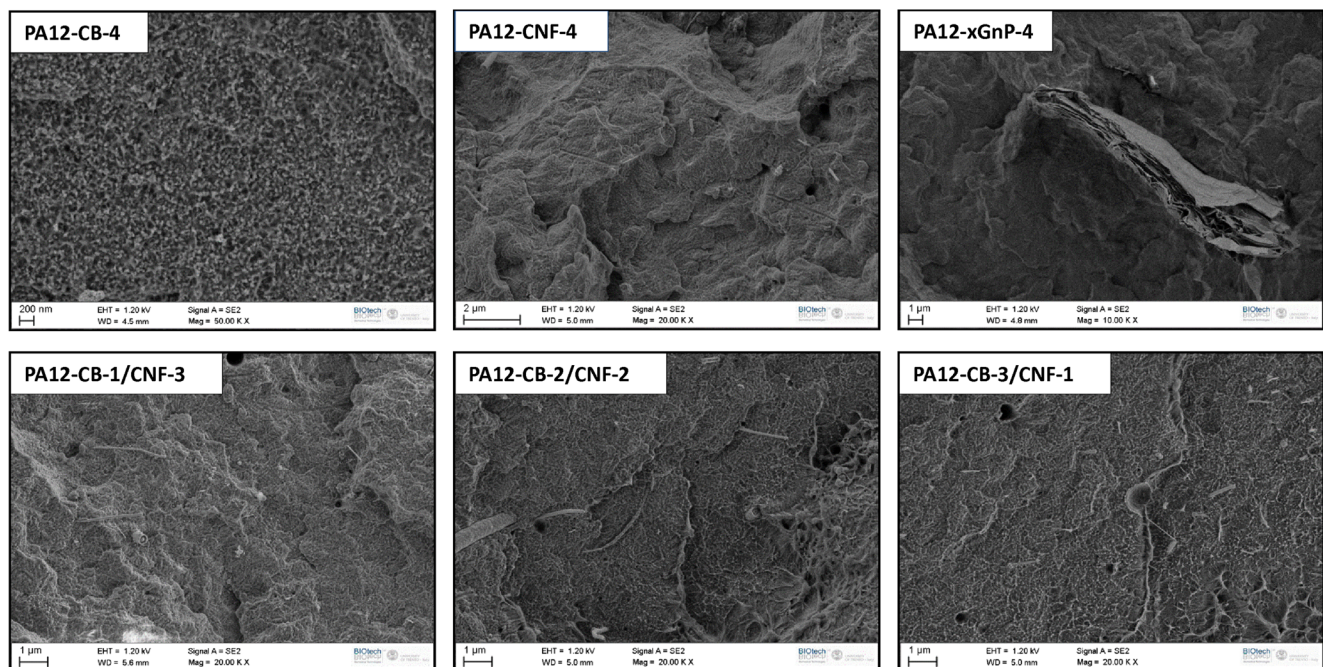


**Fig. 1** FESEM images of the fracture surface of PA12 based nanocomposites (bulk samples)

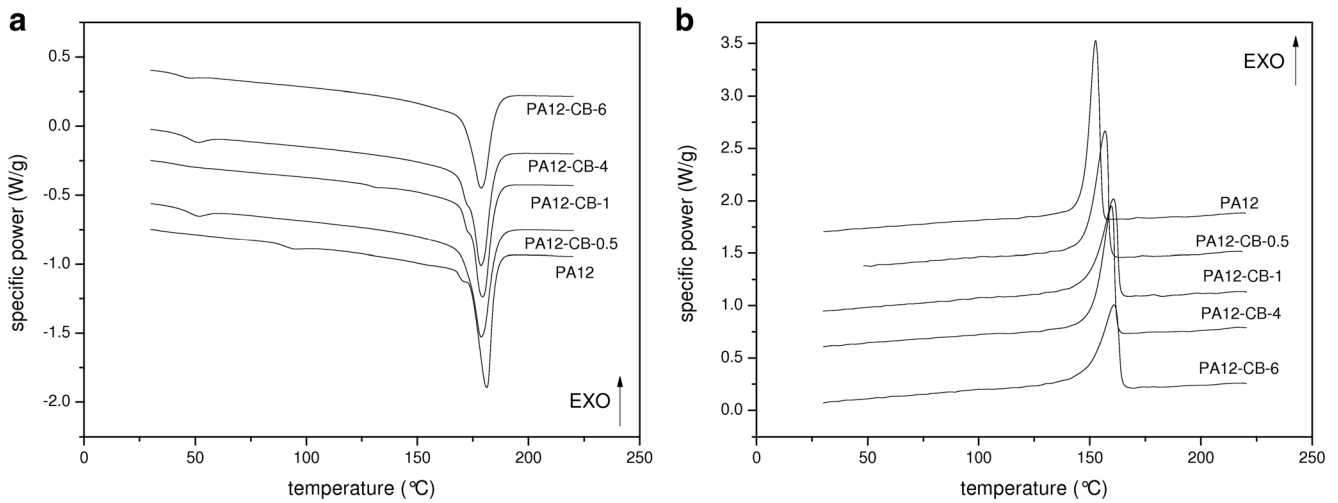


**Fig. 2** Representative DSC thermograms of CB filled nanocomposites (bulk samples). (a) First heating run, (b) cooling run

nanocomposites with different CB amounts during the first heating and the cooling scan are respectively reported, while the most important results are summarized in Table 2. It is evident that the melting temperature ( $T_m$ ) of the materials is not affected by the presence

of nanofillers nor during the first neither in the second scan (not reported for the sake of brevity). On the other hand, a slight increase of the glass transition temperature ( $T_g$ ) with respect to the neat PA12 can be detected for all the nanofilled samples, even if the trends are not proportional to the nanofiller amount. It is interesting to note that the crystallization temperature ( $T_c$ ) is systematically shifted to higher temperatures, especially at elevated filler concentrations. For instance, a  $T_c$  shift of 5 °C can be detected for the PA12-CB-6 sample. It could be therefore hypothesized that CNT acts as nucleating agent on the polymeric matrix [35]. It could be important to underline that  $T_c$  represents one of the most important parameters for the application of these materials as electro-active filters, because it determines the die-to-collector distance in the melt-blowing technology. The total crystallinity seems to be unaffected by the nanofiller introduction. Similar results were detected in our previous paper on PBT/organoclay nanocomposites [30]. The same tests were then performed on the nanocomposites containing both CB and CNF, with a total filler amount of 4%wt. As reported in Table 2, it is clear that both the melting temperature ( $T_m$ ) and the glass transition temperature ( $T_g$ ) are not substantially affected by the relative nanofiller content, and also the crystallization temperature ( $T_c$ ) and the crystalline fraction ( $X_c$ ) are not substantially influenced by the nanofiller composition.

**Table 2** Results of DSC tests on neat PA12 and relative nanocomposites (bulk samples)

Sample	$T_g$ (°C)	$T_m$ (°C)	$X_1$ (%)	$T_c$ (°C)	$X_2$ (%)
PA12	41.2	179.6	63.9	155.1	69.9
PA12-CB-0.5	41.6	179.3	65.3	158.9	64.8
PA12-CB-1	47.4	178.5	66.6	159.6	64.3
PA12-CB-4	47.7	178.7	64.4	160.6	63.7
PA12-CB-6	42.8	178.7	59.0	160.8	60.0
PA12-CNF-0.5	47.4	179.9	62.4	156.9	62.6
PA12-CNF-1	46.9	180.2	65.5	157.5	65.7
PA12-CNF-4	45.6	179.3	67.6	158.9	64.7
PA12-CNF-6	42.0	178.8	65.8	159.0	65.8
PA12-xGnP-0.5	47.3	179.9	66.9	156.6	67.1
PA12-xGnP-1	46.6	179.4	68.0	157.3	67.7
PA12-xGnP-4	45.7	178.8	68.3	157.1	67.5
PA12-xGnP-6	42.9	178.3	66.3	158.8	62.5
PA12-CB-4	47.7	178.7	64.4	160.6	63.7
PA12-CB-3/CNF-1	38.0	180.5	65.9	160.5	66.4
PA12-CB-2/CNF-2	38.2	179.0	69.6	160.0	69.6
PA12-CB-1/CNF-3	40.4	178.7	69.9	156.9	70.3
PA12-CNF-4	45.6	179.3	67.6	158.9	64.7

$T_g$  = glass transition temperature (first heating run)  
 $T_m$  = melting temperature (first heating run)  
 $X_1$  = crystallinity degree (first heating run)  
 $T_c$  = crystallization temperature (cooling run)  
 $X_2$  = crystallinity degree (cooling run)

The evaluation of the thermal degradation resistance of the prepared composites plays a key role for the intended application of these material. Thermogravimetric analysis (TGA) was therefore performed on bulk materials. In Fig. 3a representative thermograms of neat PA12 and relative CB filled nanocomposites are reported, while in Fig. 3b decomposition temperature ( $T_d$ ) values are

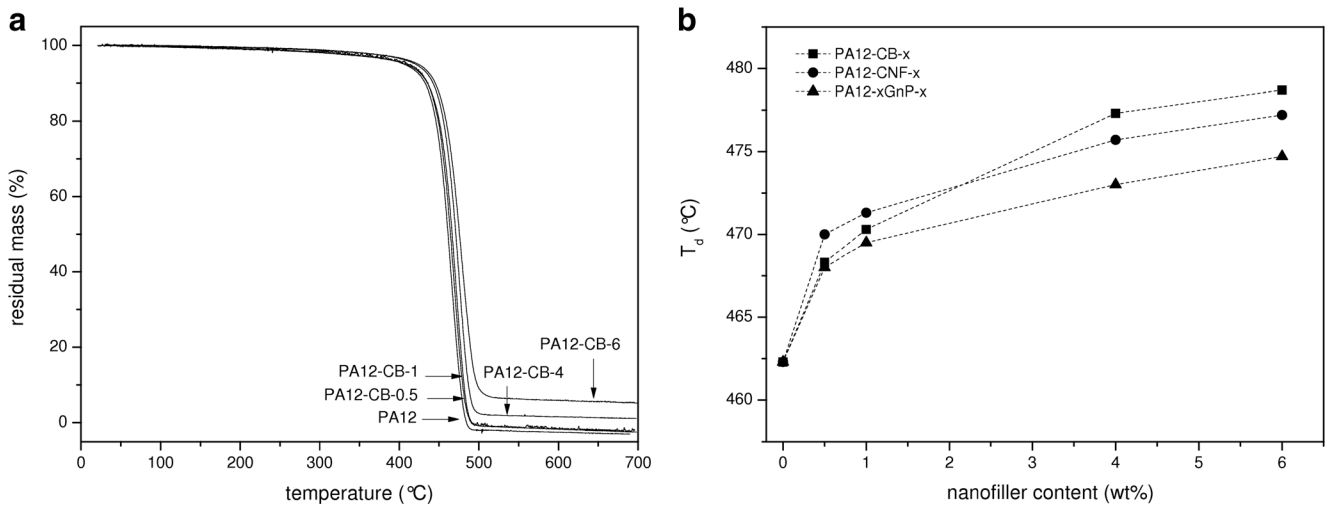


**Fig. 3** TGA tests on neat PA12 and relative nanocomposites (bulk samples). (a) Representative thermograms of CB filled nanocomposites, (b) decomposition temperature ( $T_d$ ) of nanocomposites with single nanofiller

summarized. It is evident that all the prepared composites show a single degradation step located at about 470 °C, and the mass residue at 700 °C is proportional to the filler loading. Regardless to the nanofiller type, from Fig. 3b it is clear that the introduction of carbonaceous nanofillers determines a substantial enhancement of the decomposition temperature, proportionally to the filler loading. For instance, a  $T_d$  increment of 16 °C with respect to the neat PA12 can be observed for the PA12-CB-6 composite. TGA tests on nanocomposite samples containing both CNF and CB (not reported for the sake of brevity) do not show any synergistic effect promoted by the addition of both nanofillers. The observed increment in the thermal degradation resistance of the nanocomposite samples is in agreement with several studies present in literature [36]. In fact, Gedler et al. reported that well dispersed graphite nanoplatelets improved the thermal stability of polycarbonate foams due to their barrier effect, delaying the diffusion of volatile products during the degradation process. In fact, graphene nanoplatelets created a tortuous path for air, thus delaying the thermo-oxidative degradation of the material [37].

The effect played by nanofiller introduction on the dimensional stability and on the mechanical resistance of the prepared composites is an important aspect in the present investigation. In Fig. 4a representative stress-strain curves of CB filled nanocomposites is shown, while the trends of the elastic and failure properties of the composites as a function of the filler loading are reported in Fig. 4b–d. It is immediately evident that nanofiller addition promotes a substantial increment of the elastic modulus, proportionally to the filler loading. As already observed in our previous work on poly(cyclooctene) (PCO) based nanocomposites [12],

xGnP seems to be more effective in increasing the stiffness of the material. For instance, with a xGnP concentration of 6 wt% it is possible to enhance the elastic modulus of about 40% with respect to neat PA12. As it can be easily observed in Fig. 4a, nanofiller introduction promotes an heavy embrittlement of the samples, with a reduction of the maximum stress ( $\sigma_{max}$ ) and of the strain at the maximum stress values ( $\epsilon_{max}$ ) (see Fig. 4c and d). The observed reduction of the failure properties is probably due to the partial aggregation of the nanofillers within the matrix. In order to detect possible synergistic effects promoted by the addition of both CB and CNF, also nanocomposites with mixed composition were investigated. As reported in Fig. 4e, an important negative deviation of the elastic modulus values from the rule of mixture can be detected, especially with a CNF/CB relative ratio of 50%, while maximum stress values seem to substantially follow the theoretical predictions (see Fig. 4f).

The possibility of utilize these nanocomposites as electrically heated devices depend on their electrical conductivity. Therefore, electrical resistivity measurements were performed. In Fig. 5a bulk resistivity values as a function of the filler loading are shown. The introduction of carbon based nanofiller in the insulating polymeric matrix increases the electrical conductivity values. As an example, a resistivity value lower than  $10^3 \Omega \text{ cm}$  can be achieved with a CB content of 6%wt. It is possible to see that CB introduction confers a good conductivity to the samples and it is possible to appreciate a lower electrical percolation threshold in these samples (3 wt%) with respect to CNF and xGnP filled nanocomposites. On the other hand, only with a xGnP amount higher than 4%wt the electrical

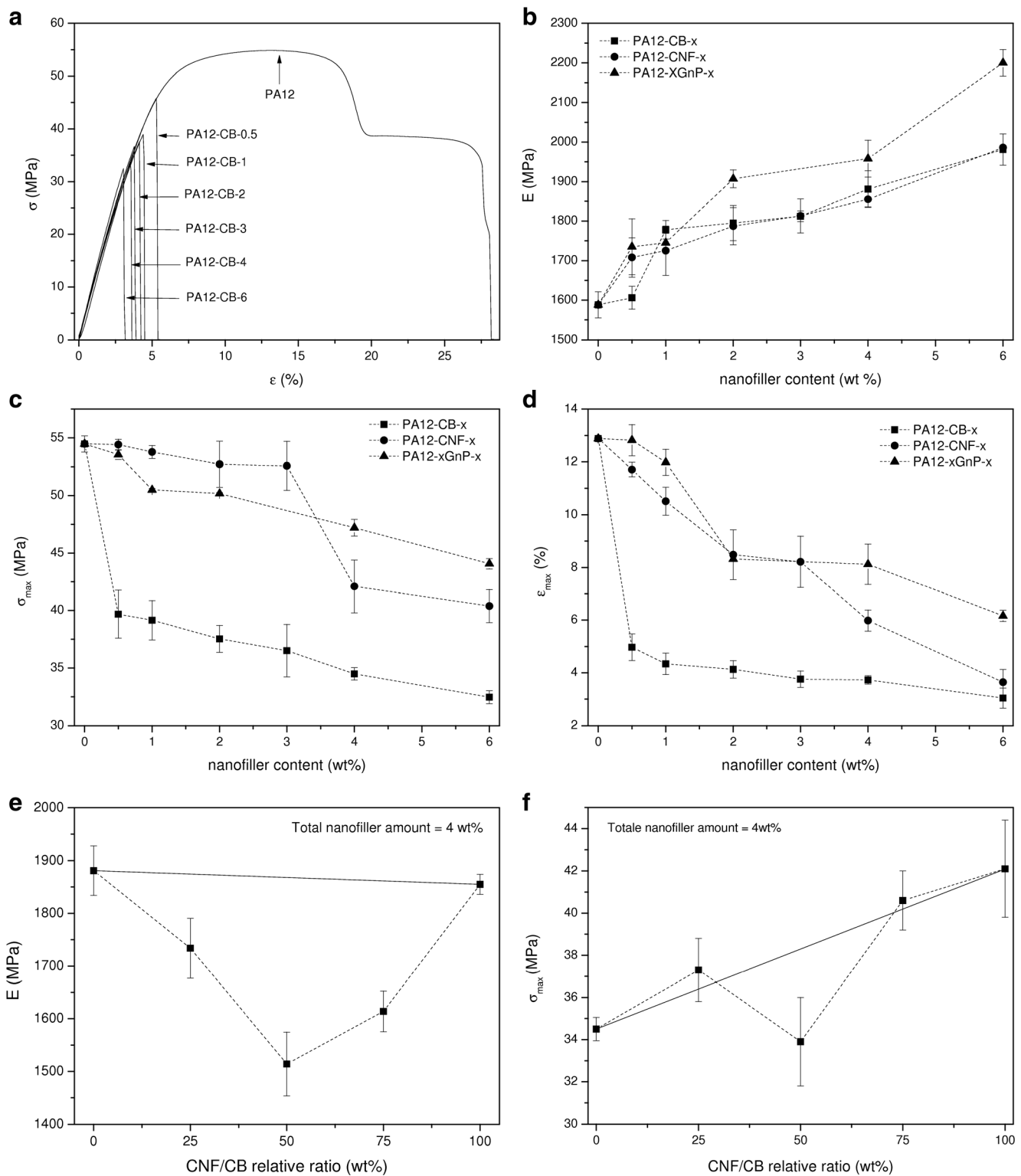


**Fig. 4** Quasi-static tensile properties of PA12 based nanocomposites (bulk samples). (a) Representative stress-strain curves of CB filled nanocomposites, (b) elastic modulus, (c) maximum stress and (d) strain at

maximum stress of nanocomposites with a single filler. (e) Elastic modulus and (f) maximum stress of nanocomposites with different CNF/CB ratios (total filler amount 4 wt%)

percolation threshold is reached. As already observed in our previous paper on PCO based nanocomposites [12], CB is more effective in increasing the conductivity of

the materials, while for xGnP filled samples an higher filler amount is required to obtain low resistivity values. In order to take advantage of the synergistic effect

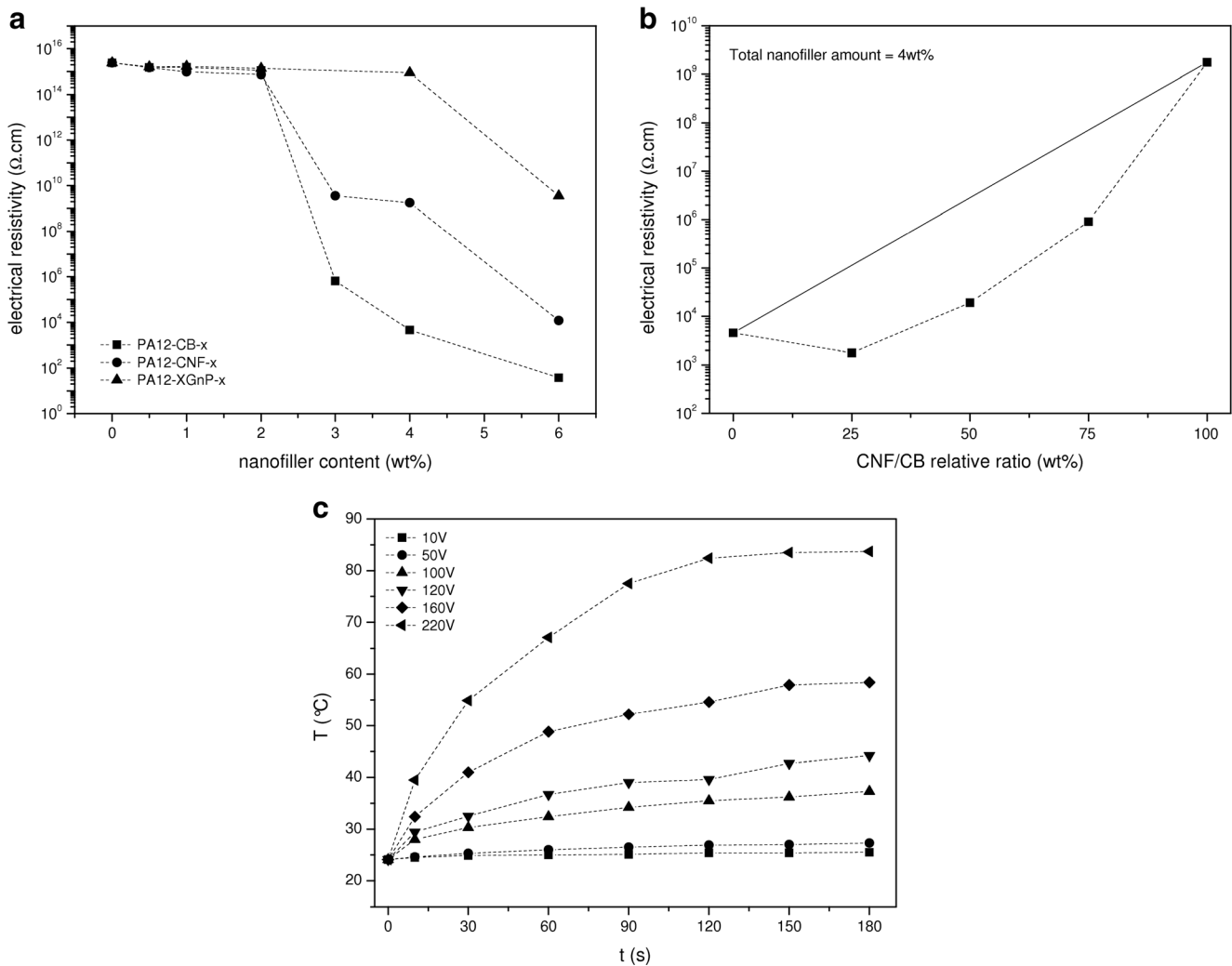


**Fig. 5** Electrical properties of PA12 based nanocomposites (*bulk samples*). (a) Electrical resistivity of nanocomposites with a single nanofiller and of (b) nanocomposites with different CNF/CB ratios (total

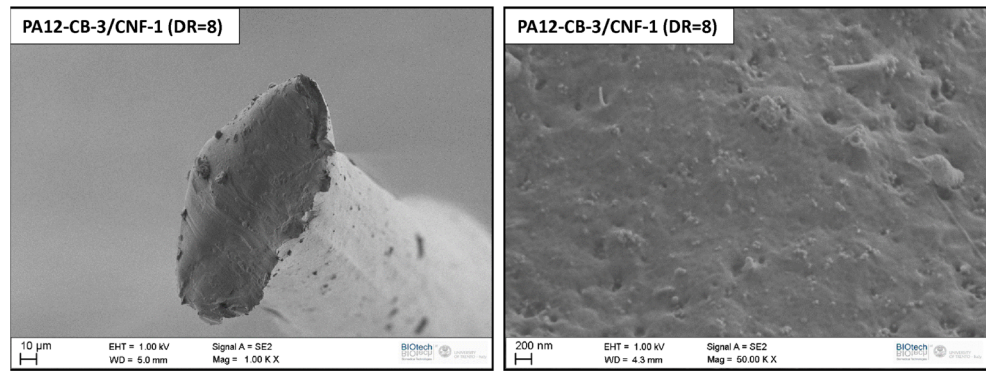
filler amount 4 wt%). (c) Surface temperature evolution upon voltage application of the PA12-CB-3/CNF-1 nanocomposite sample

promoted by the simultaneous of CNF and CB nanofillers, samples with a total filler concentration of 4%wt at different CNT/CB relative amounts were prepared and electrically characterized (see Fig. 5b). From this set of data it is possible to understand that the resistivity decreases with a non-linear trend, reaching thus resistivity values that could not be achieved with a single nanofiller. As an example, for the PA12-CB-3/CNF-1 nanocomposite it is possible to obtain an electrical resistivity of  $1.8 \times 10^3 \Omega \text{ cm}$ . According to the indication of the industrial partner (UFI Innovation Center Srl), a target resistivity value equal or lower than  $10^3 \Omega \text{ cm}$  is required to prepare nanocomposite filters that could be effectively heated through Joule effect [38]. After this characterization on the bulk materials, the PA12-CB-3/CNF-1 nanocomposite sample can be detected as the best compromise to reach good electrical

conductivity values without seriously impairing the failure properties of the materials. It is also important to underline that increasing the filler amount above the 4 wt% the viscosity of the matrix at the molten state is noticeably increased. In these conditions, the processability of these materials through melt blowing technology would be compromised.

The heating capability of bulk nanocomposites was evaluated through a thermocamera, and in Fig. 5c the evolution of the surface temperature upon voltage application of PA12-CB-3/CNF-1 nanocomposite is reported. It can be easily noticed how an effective heating can be detected for applied voltages higher than 100 V. Obviously, the higher the voltage, the higher the temperature reached. The most interesting aspect is that during the first seconds a rapid temperature increase occurs, and the material reaches a temperature plateau

**Fig. 6** FESEM images of the fracture surface of the PA12-CB-3/CNF-1 fiber (draw ratio = 8)



after 120 s. For instance, with a voltage of 220 V it is possible to increase the surface temperature up to 82 °C after 180 s. This aspect is very important for the final application of these materials as electro-active filters, because the thermal degradation of the materials for prolonged voltage application times should be avoided.

### Characterization of the fibers

The investigation of the physical properties of bulk materials allowed the determination of the most promising compositions for the intended application. Therefore, neat PA12 and PA12-CB-3/CNF-1 nanocomposite fibers were prepared and drawn applying different draw ratios. Furthermore, PA12-CB-10 were also prepared, in order to detect the effect of the nanofiller addition at the maximum filler loading achievable from a technological point of view (for higher filler contents the viscosity of the matrix would be too high also for a common extrusion process). The investigation of the microstructural behaviour of the prepared fiber needs to be investigated, in order to correlate the morphology of the fibers with their physical properties. In Fig. 6 representative FESEM images of the fracture surface of the PA12-CB-3/CNF-1 fiber produced at a draw ratio equal to 8 are reported. In FESEM image at lower magnification it is difficult to distinguish the presence of the nanofiller, while from the micrograph of the cross section of the fiber at higher magnification it is possible to detect the presence of CB agglomerates homogeneously distributed within the matrix. Interestingly, the dimension of these aggregates (30–40 nm) is noticeably reduced with respect to that shown in the corresponding bulk materials (see Fig. 1). As reported in our previous paper on polyethylene nanocomposite fibers [39], the drawing process produced the rupture of CB aggregates and, most probably, their alignment along the drawing direction. This means that the agglomerates of CB nanoparticles, once exposed to an elongational flow in the solid state, orient themselves along the strain direction. Unlike

conventional microfillers, CB aggregates can be deformed and fractured to form long streams of nanoparticles dispersed within the polymer matrix. This process is very similar to the exfoliation process induced by the flow in polymer/clay nanocomposites with a good affinity between the two components [40].

The tensile properties of the nanocomposite fibers were measured and compared with those of the unfilled fibers. In Fig. 7a the elastic modulus values of neat PA12 and PA12-CB-3/CNF-1 fibers as a function of the draw ratio are reported, while in Fig. 7b and in c the stress at break (UTS) and strain at break values ( $\epsilon_{UTS}$ ) are respectively reported. It is interesting to note how the alignment of CB aggregates along the drawing direction promotes a systematic increase of the elastic modulus over the whole range of applied draw ratios. Also the tensile strength of the fibers is slightly increased upon nanofiller addition. It is also important to note that the observed improvements of the tensile properties of the fibers have been obtained without impairing the strain at break values. Similar trends were observed in our previous work on polyethylene nanocomposite fibers [39].

The evaluation of the electrical conductivity of the prepared fibers is of fundamental importance for the preparation of electro-active melt blown filters. Therefore, in Table 3 electrical conductivity values of neat PA12 and PA12-CB-3/CNF-1 fibers were compared with the corresponding bulk materials. For as concerns bulk materials, it has been already shown that nanofiller addition promotes a strong decrease of the electrical resistivity up to  $1.8 \times 10^3 \Omega \text{ cm}$  (see Fig. 5b). It is interesting to note how the extrusion process followed by the subsequent drawing operations promotes an enhancement of the electrical resistivity. For neat PA12, the observed resistivity increment is rather limited, while for the PA12-CB-3/CNF-1 nanocomposite fiber a resistivity increase of about two order of magnitude can be registered. In order to obtain nanofilled fibers with resistivity values lower than the target values proposed

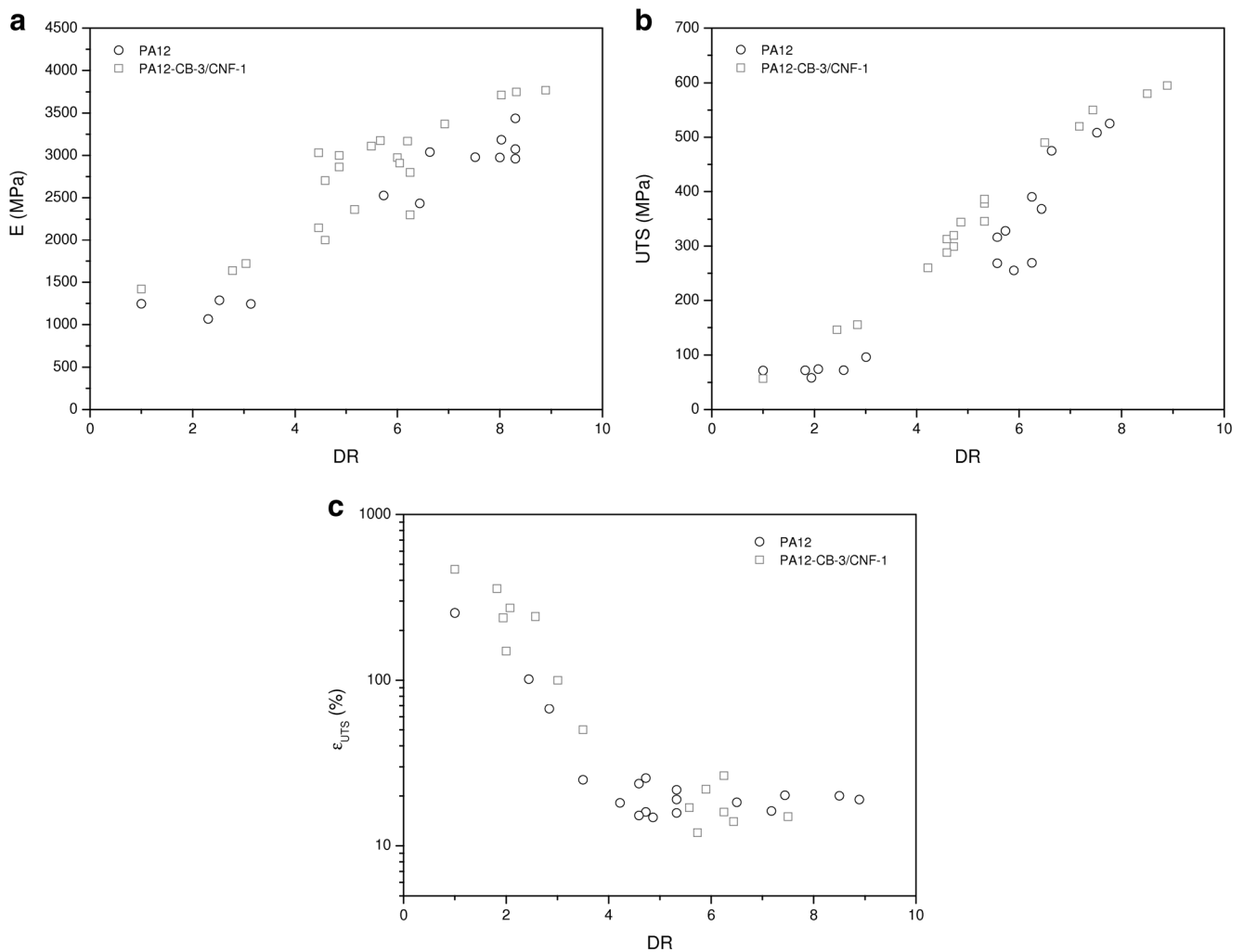


**Fig. 7** Tensile properties of neat PA12 and PA12-CB-3/CNF-1 fibers as a function of the draw ratio. **(a)** Elastic modulus, **(b)** stress at break and **(c)** strain at break

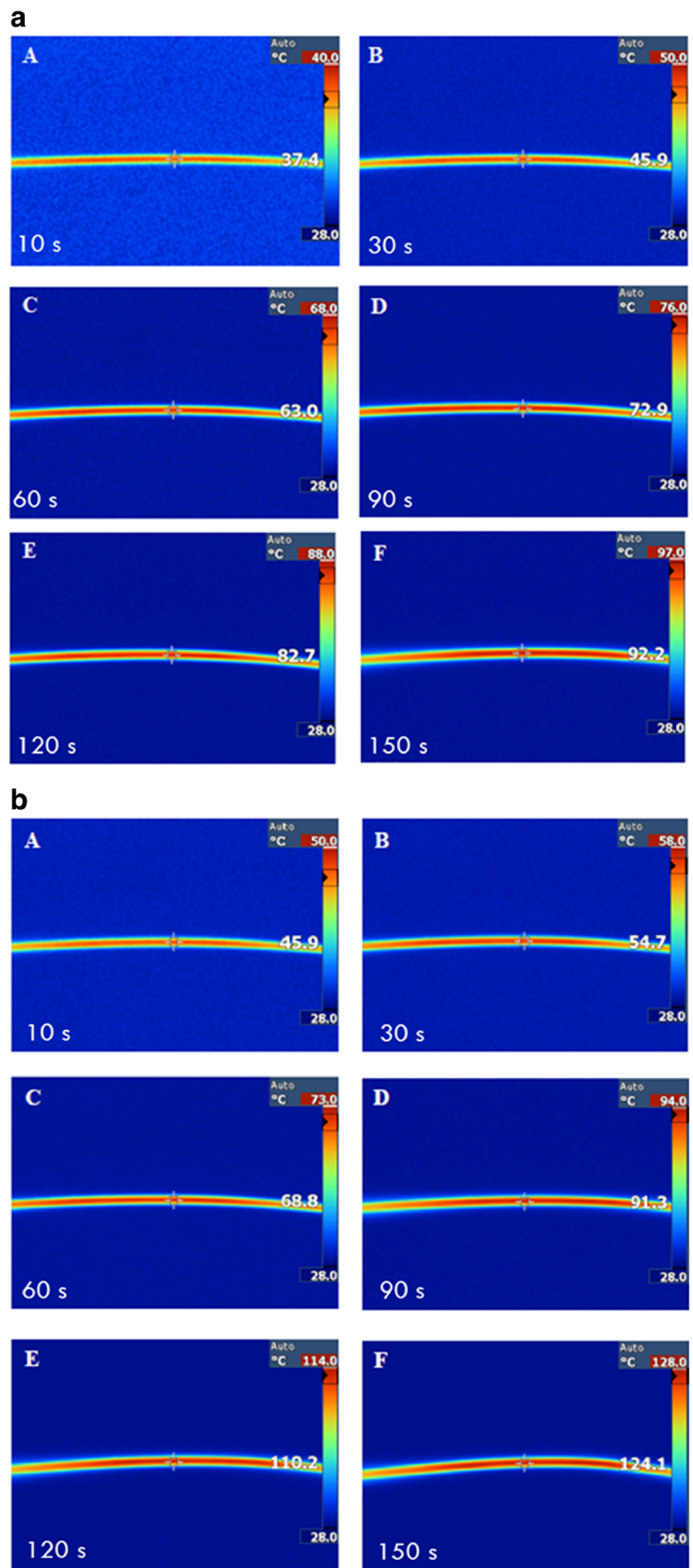
by UFI innovation center (i.e.  $10^3 \Omega \text{ cm}$ ), a much higher nanofiller amount is required (i.e. 10 wt%, see Table 2). A possible explanation of this result can be found in our previous paper on poly(lactic acid) based nanocomposites [41]. In that work it was demonstrated how carbonaceous nanofiller orient itself along the extrusion/drawing direction, and only at higher filler

contents nanofiller aggregates will start contacting each other forming a conductive network within the polymer, thus decreasing the electrical resistivity. On the other hand, the random filler orientation observed in bulk materials facilitates the formation of the conductive network at much lower filler contents with respect to the corresponding fibers. The negative influence played by the extrusion process on the electrical conductivity of the nanocomposite fibers explains why it is not possible to heat PA12-CB-3/CNF-1 nanocomposite fibers upon the application of a voltage through the Joule effect. Only PA12-CB-10 nanocomposite fibers show interesting heating capabilities once a voltage is applied (see Fig. 8(a-b)). With a potential of 100 V, it is possible to reach a temperature of 92 °C after 150 s, while with 220 V a higher temperature (i.e. 124 °C) can be reached in the same time interval. These results confirm the potential of the prepared fibers to be applied in

**Table 3** Comparison of electrical resistivity values of neat PA12 and relative nanocomposites (bulk and fiber samples)

Sample	Bulk	Fiber (DR = 8)
	$\rho$ ( $\Omega \text{ cm}$ )	$\rho$ ( $\Omega \text{ cm}$ )
PA12	$2.4 \cdot 10^{15}$	$1.0 \cdot 10^{15}$
PA12-CB-3/CNF-1	$1.8 \cdot 10^3$	$1.0 \cdot 10^5$
PA12-CB-10	-	$1.0 \cdot 10^2$

**Fig. 8** IR thermograms representing the surface temperature evolution upon voltage application of PA12-CB-10 nanocomposite fiber. Applied voltage of (a) 100 V and (b) 220 V



electro-active filters, but further efforts will be required to lower their electrical percolation threshold, increasing thus their heating capability even at limited voltage levels.

## Conclusions

Novel polyamide 12 based nanocomposites filled with different amounts of carbonaceous nanofillers were prepared through melt compounding and thermo-electrically characterized. The physical properties of bulk materials were then compared with those of the corresponding fibers.

FESEM micrographs demonstrated that both CB and CNF nanofillers were homogeneously dispersed in the matrix, while an evident aggregation was detected in xGnP nanocomposites. DSC tests evidenced a slight increase of the glass transition temperature and of the crystallization temperature, and also the thermal degradation temperature was enhanced upon nanofiller addition. Nanofiller introduction promoted a substantial increment of the elastic modulus coupled with an heavy embrittlement of the samples. Electrical resistivity values lower than  $10^3 \Omega \text{ cm}$  were achieved with a CB content of 6%wt, and interesting synergistic effects were detected in nanocomposites filled with both CB and CNF.

FESEM images on nanocomposite fibers demonstrated how the drawing process produced the rupture of CB aggregates and their alignment along the drawing direction, thus promoting a systematic increase of the elastic modulus and of the tensile strength with respect to the unfilled fibers. As a drawback, the extrusion/drawing operations promoted an electrical resistivity enhancement of two orders of magnitude with respect to the corresponding bulk materials, and a much higher nanofiller amount was thus required to obtain an effective surface heating upon voltage application.

**Acknowledgements** This research activity has been supported by Fondazione Cassa di Risparmio di Trento e Rovereto (CARITRO) within the project "Bando Caritro 2014 per progetti di ricerca scientifica finalizzati allo sviluppo di iniziative imprenditoriali". The work was also supported by the National Interuniversity Consortium of Materials Science and Technology (INSTM). Mrs. Daniela Fronterre is gratefully acknowledged for her collaboration to the experimental activities.

## References

- Agag T, Koga T, Takeichi T (2001) Studies on thermal and mechanical properties of polyimide-clay nanocomposites. *Polymer* 42(8):3399–3408
- Rong M, Zhang M, Zheng Y (2001) Improvement of tensile properties of nano-SiO<sub>2</sub>/PP composites in relation to percolation mechanism. *Polymer* 42(7):3301–3304
- Fu X, Qutubuddin S (2000) Synthesis of polystyrene-clay nanocomposites. *Mater Lett* 42:12–15
- Shelley JS, Mather PT, De Vries KL (2001) Reinforcement and environmental degradation of nylon-6/clay nanocomposites. *Polymer* 42(13):5849–5858
- Shu Z, Chen G, Qi Z (2000) Polymer/clay nano-composite and its unique flame retardance. *Plastics Industry* 28(3):24–26
- Uhl FM, Wilkie CA (2002) Polystyrene/graphite nanocomposites: effect on thermal stability. *Polym Degrad Stab* 76(1):111–122
- Norman RH, Boonstra BB (1972) Conductive rubbers and plastics. *J Polym Sci Part B : Polym Lett* 10:479
- Armad M (1990) Polymers with ionic conductivity. *Adv Mater* 2: 278–286
- Ibidapo TA (1988) Classification of ionic polymers. *Polym Eng Sci* 28:1473–1476
- Biani A, Dorigato A, Bonani W, Slouf M, Pegoretti A. Mechanical behaviour of cyclic olefin copolymer/exfoliated graphite nanoplatelets nanocomposites foamed through supercritical carbon dioxide. *Express Polym Lett*. Accepted 01/07/2016
- Dorigato A, Giusti G, Bondioli F, Pegoretti A (2013) Electrically conductive epoxy nanocomposites containing carbonaceous fillers and in-situ generated silver nanoparticles. *Express Polym Lett* 7(8): 673–682
- Dorigato A, Pegoretti A (2017) Effects of carbonaceous nanofillers on the mechanical and electrical properties of crosslinked poly(cyclooctene). *Polym Eng Sci* 57:537–543
- Pedrazzoli D, Dorigato A, Pegoretti A (2012) Monitoring the mechanical behaviour of electrically conductive polymer nanocomposites under ramp and creep conditions. *J Nanosci Nanotechnol* 12(5):4093–4102
- Pedrazzoli D, Dorigato A, Pegoretti A (2012) Monitoring the mechanical behaviour under ramp and creep conditions of electrically conductive polymer composites. *Compos A : Appl Sci Manuf* 43: 1285–1292
- Maiti A, Svizhenko A, Anantram MP (2002) Electronic transport through carbon nanotubes: effects of structural deformation and tube chirality. *Phys Rev Lett* 88(12):126805
- Ou R, Gerhardt RA, Marrett C, Moulart A, Colton JS (2003) Assessment of percolation and homogeneity in ABS/carbon black composites by electrical measurements. *Compos Part B : Eng* 34(7):607–614
- Terranova ML, Orlanducci S, Fazi E, Sessa V, Piccirillo S, Rossi M, Manno D, Serra A (2003) Organization of single-walled nanotubes into macro-sized rectangularly shaped ribbons. *Chem Phys Lett* 381(1–2):86–93
- Chanda M, Roy SK (2007) *Plastics technology Handbook*, 4th edn. CRC Press, Boca Raton
- Kohan MI (1995) *Nylon plastics Handbook*. Carl Hanser Verlag, Munich
- Bashford D (1997) *Thermoplastics: directory and Databook*. Springer, London
- Jose S, Nair SV, Thomas S, Karger-Kocsis J (2006) Effect of reactive Compatibilisation on the phase morphology and tensile properties of PA12/PP blends. *J Appl Polym Sci* 99:2640–2660
- Tang T, Lei Z, Huang B (1996) Studies on morphology and crystallization of polypropylene/polyamide 12 blends. *Polymer* 37: 3219–3226
- Sarkissova M, Harrats C, Groeninckx G, Thomas S (2004) Design and characterisation of microfibrillar reinforced composite materials based on PET/PA12 blends composites part a : applied Science and manufacturing 35:489–499.
- Alexandre B, Langevin D, Mederic P, Aubry T, Couderc H, Nguyen QT, Saiter A, Marais S (2009) Water barrier properties of polyamide 12/montmorillonite nanocomposite membranes: structure and volume fraction effects. *J Membr Sci* 328:186–204
- Alexandre B, Marais S, Langevin D, Mederic P, Aubry T (2006) Nanocomposite-based polyamide 12/montmorillonite :

- relationships between structures and transport properties. *Desalination* 199:164–166
26. Hasook A, Muramatsu H, Tanoue S, Iemoto Y, Unryu T (2008) Preparation of nanocomposites by melt compounding Poly(lactic acid)/polyamide 12/Organoclay at different screw rotating speeds using a twin screw extruder. *Polym Compos* 29:1–8
  27. Zhang Y, Yang JH, Ellis TS, Shi J (2006) Crystal structures and their effects on the properties of polyamide 12/clay and polyamide 6–polyamide 66/clay nanocomposites. *J Appl Polym Sci* 100:4782–4794
  28. Dorigato A, Fambri L (2011) Thermo-mechanical behaviour of polyamide 12 - polyamide 66 recycled fibers composites. *Polym Compos* 32:786–795
  29. Dorigato A, Fambri L (2013) Effect of aramid regenerated fibers on thermo-mechanical behaviour of polyamide 12 composites. *J Reinf Plast Compos* 32:1243–1256
  30. Dorigato A, Brugnara M, Giacomelli G, Fambri L, Pegoretti A (2016) Thermal and mechanical behaviour of innovative melt-blown fabrics based on polyamide nanocomposites. *J Ind Text* 45(6):1504–1515
  31. Athreya SR, Kalaitzidou K, Das S (2010) Processing and characterization of a carbon black-filled electrically conductive nylon-12 nanocomposite produced by selective laser sintering. *Mater Sci Eng A* 527(10–11):2637–2642
  32. Yanagizawa H, Kodaira T (2004) Dependence of electrical conductivities of carbon black filled nylon-12 fibers on spinning conditions. *Sen-I-Gaikkaishi* 60:203–212
  33. Mehta RH (1999) Physical constants of various polyamides. In: Brandrup J, Immergut EH, Grulke EA (eds) *polymers Handbook* 4th Ed., vol 1. Wiley-Interscience, Hoboken, p V/126.
  34. Medalia AI, Heckman FA (1969) Morphology of aggregates II. Size and shape factors of carbon black aggregates from electron microscopy. *Carbon* 7(5):567–582
  35. Lazzeri A, Zebarjad SM, Pracella M, Cavalier K, Rosa R (2005) Filler toughening of plastics. Part 1 - the effect of surface interactions on physico-mechanical properties and rheological behaviour of ultrafine CaCO<sub>3</sub>/HDPE nanocomposites. *Polymer* 46(3):827–844
  36. Dorigato A, Pegoretti A, Quaresimin M (2011) Thermo-mechanical characterization of epoxy/clay nanocomposites as matrices for carbon/nanoclay/epoxy laminates. *Mater Sci Eng A* 528(19–20):6324–6333
  37. Gedler G, Antunes M, Realinho V, Velasco J (2012) Thermal stability of polycarbonate-graphene nanocomposite foams. *Polym Degrad Stab* 97(8):1297–1304
  38. Dorigato A, Brugnara M, Pegoretti A (2017) Synergistic effects of carbon black and carbon nanotubes on the electrical resistivity of poly(butylene-terephthalate) nanocomposites. *Adv Polym Technol*. doi:10.1002/adv.21833
  39. D'Amato M, Dorigato A, Fambri L, Pegoretti A (2012) High performance polyethylene nanocomposite fibers. *Express Polym Lett* 6(12):954–964
  40. Tokihisa M, Yakemoto K, Sakai T, Utracki LA, Sepehr M, Li J, Simard Y (2006) Extensional flow mixer for polymer nanocomposites. *Polym Eng Sci* 46:1040–1050
  41. Tait M, Pegoretti A, Dorigato A, Kaladzidou K (2011) The effect of filler type and content and the manufacturing process on the performance of multifunctional carbon/poly-lactide composites. *Carbon* 49:4280–4290